

Indications of Neutrino Oscillation in a 250 km Long-baseline Experiment

M.H.Ahn,¹ S.Aoki,² H.Bhang,¹ S.Boyd,^{3,*} D.Casper,⁴ J.H.Chi,⁵ S.Fukuda,⁶ Y.Fukuda,^{6,*} W.Gajewski,⁴ T.Hara,² M.Hasegawa,⁷ T.Hasegawa,⁸ Y.Hayato,⁹ J.Hill,^{10,*} A.K.Ichikawa,⁹ A.Ikeda,¹¹ T.Inagaki,⁷ T.Ishida,⁹ T.Ishii,⁹ M.Ishitsuka,⁶ Y.Itow,⁶ T.Iwashita,² H.I.Jang,^{5,*} J.S.Jang,⁵ E.J.Jeon,⁹ C.K.Jung,¹⁰ T.Kajita,⁶ J.Kameda,⁶ K.Kaneyuki,⁶ I.Kato,⁷ E.Kearns,¹² A.Kibayashi,¹³ D.Kielczewska,^{14,15} K.Kobayashi,⁶ B.J.Kim,¹ C.O.Kim,¹⁶ J.Y.Kim,⁵ S.B.Kim,¹ T.Kobayashi,⁹ M.Kohama,² Y.Koshio,⁶ W.R.Kropp,⁴ J.G.Learned,¹³ S.H.Lim,⁵ I.T.Lim,⁵ H.Maesaka,⁷ K.Martens,^{10,*} T.Maruyama,^{9,*} S.Matsuno,¹³ C.Mauger,^{10,*} C.Mcgrew,¹⁰ S.Mine,⁴ M.Miura,⁶ K.Miyano,¹⁷ S.Moriyama,⁶ M.Nakahata,⁶ K.Nakamura,⁹ I.Nakano,¹¹ F.Nakata,² T.Nakaya,⁷ S.Nakayama,⁶ T.Namba,⁶ K.Nishikawa,⁷ S.Nishiyama,² S.Noda,² A.Obayashi,⁶ A.Okada,⁶ T.Ooyabu,⁶ Y.Oyama,⁹ M.Y.Pac,¹⁸ H.Park,¹ M.Sakuda,⁹ N.Sakurai,⁶ N.Sasao,⁷ K.Scholberg,¹⁹ E.Sharkey,¹⁰ M.Shiozawa,⁶ H.So,¹ H.W.Sobel,⁴ A.Stachyra,³ J.L.Stone,¹² Y.Suga,² L.R.Sulak,¹² A.Suzuki,² Y.Suzuki,⁶ Y.Takeuchi,⁶ N.Tamura,¹⁷ T.Toshito,^{6,*} Y.Totsuka,^{6,9} M.R.Vagins,⁴ C.W.Walter,¹² R.J.Wilkes,³ S.Yamada,⁶ S.Yamamoto,⁷ C.Yanagisawa,¹⁰ H.Yokoyama,²⁰ J.Yoo,¹ M.Yoshida,⁹ and J.Zalipska¹⁵

(The K2K Collaboration)

¹ Department of Physics, Seoul National University, Seoul 151-742, KOREA

² Kobe University, Kobe, Hyogo 657-8501, JAPAN

³ Department of Physics, University of Washington, Seattle, WA 98195-1560, USA

⁴ Department of Physics and Astronomy, University of California, Irvine, Irvine, CA 92697-4575, USA

⁵ Department of Physics, Chonnam National University, Kwangju 500-757, KOREA

⁶ Institute for Cosmic Ray Research, University of Tokyo, Kashiwa, Chiba 277-8582, JAPAN

⁷ Department of Physics, Kyoto University, Kyoto 606-8502, JAPAN

⁸ Research Center for Neutrino Science, Tohoku University, Sendai, Miyagi 980-8578, JAPAN

⁹ Institute of Particle and Nuclear Studies, KEK, Tsukuba, Ibaraki 305-0801, JAPAN

¹⁰ Department of Physics and Astronomy, State University of New York, Stony Brook, NY 11794-3800, USA

¹¹ Department of Physics, Okayama University, Okayama, Okayama 700-8530, JAPAN

¹² Department of Physics, Boston University, Boston, MA 02215, USA

¹³ Department of Physics and Astronomy, University of Hawaii, Honolulu, HI 96822, USA

¹⁴ Institute of Experimental Physics, Warsaw University, 00-681 Warsaw, POLAND

¹⁵ A. Soltan Institute for Nuclear Studies, 00-681 Warsaw, POLAND

¹⁶ Department of Physics, Korea University, Seoul 136-701, KOREA

¹⁷ Department of Physics, Niigata University, Niigata, Niigata 950-2181, JAPAN

¹⁸ Department of Physics, Dongshin University, Naju 520-714, KOREA

¹⁹ Department of Physics, Massachusetts Institute of Technology, Cambridge, MA 02139, USA

²⁰ Department of Physics, Tokyo University of Science, Noda, Chiba 278-0022, JAPAN

(Dated: May 21, 2019)

The K2K experiment observes indications of neutrino oscillation: a reduction of ν_μ flux together with a distortion of the energy spectrum. Fifty-six beam neutrino events are observed in Super-Kamiokande (SK), 250 km from the neutrino production point, with an expectation of $80.1^{+6.2}_{-5.4}$. Twenty-nine one ring μ -like events are used to reconstruct the neutrino energy spectrum, which is better matched to the expected spectrum with neutrino oscillation than without. The probability that the observed flux at SK is explained by statistical fluctuation without neutrino oscillation is less than 1%.

PACS numbers: PACS numbers: 14.60.Pq, 13.15.+g, 23.40.Bw, 95.55.Vj

Recent atmospheric and solar neutrino data indicate the existence of neutrino oscillation and therefore the existence of neutrino mass [1, 2, 3]. The zenith angle distribution of atmospheric neutrinos observed by Super-Kamiokande (SK) shows a clear deficit of upward-going muon neutrinos, which is well explained by two-flavor ν_μ - ν_τ oscillations with Δm^2 around 3×10^{-3} eV 2 , and $\sin^2 2\theta$ close to or equal to unity.

The KEK to Kamioka long-baseline neutrino oscillation experiment (K2K) [4] uses an accelerator-produced neutrino beam with a neutrino flight distance of 250 km

to probe the same Δm^2 region as that explored with atmospheric neutrinos. The neutrino beam is produced by a 12 GeV proton beam from the KEK proton synchrotron. After hitting an aluminum target, the positively charged particles, mainly pions, are focused by a pair of pulsed magnetic horns [5]. The neutrinos produced from the decays of these particles are 98% pure muon neutrinos with a mean energy of 1.3 GeV.

This analysis is based on data taken from June 1999 to July 2001, corresponding to 4.8×10^{19} protons on target (POT). The pion momentum and angular distributions

downstream of the second horn are occasionally measured with a gas-Cherenkov detector (PIMON) [6] in order to verify the beam Monte Carlo (MC) simulation and to estimate the errors on the flux prediction at SK. The direction of the beam is monitored on a spill-by-spill basis by observing the profile of the muons from the pion decays with a set of ionization chambers and silicon pad detectors located just after the beam dump. The neutrino beam itself is measured in a set of near neutrino detectors (ND) located 300 m from the proton target. The measurements made at the ND are used to verify the stability and the direction of the beam, and to determine the flux normalization and the energy spectrum before the neutrinos travel the 250 km to SK. The flux at SK is estimated from the flux of the ND by multiplying the Far/Near (F/N) ratio, the ratio of fluxes between the far detector(SK) and ND, to that of the ND.

Since both a suppression in the number of events and a distortion of the spectrum are expected for neutrinos which travel a fixed path length in the presence of oscillations, both the number of observed events and the spectral shape information at SK are compared with expectation. All of the beam-induced neutrino events observed within the fiducial volume of SK are used to measure the overall suppression of flux. In order to study the spectral distortion, 1 ring μ -like events ($1R\mu$) are selected to enhance the fraction of charged-current (CC) quasi-elastic (QE) interactions ($\nu_\mu + n \rightarrow \mu + p$). Only the muon is visible in these reactions since the proton momentum is typically below Cherenkov threshold. The energy of the parent neutrino can be calculated by using the observed momentum of the muon, assuming QE interactions, and neglecting Fermi momentum:

$$E_\nu^{\text{rec}} = \frac{m_N E_\mu - m_\mu^2/2}{m_N - E_\mu + P_\mu \cos \theta_\mu}, \quad (1)$$

where m_N , E_μ , m_μ , P_μ and θ_μ are the nucleon mass, muon energy, the muon mass, the muon momentum and the scattering angle relative to the neutrino beam direction, respectively.

The ND is comprised of two detector systems: a 1 kiloton water Cherenkov detector (1KT) and a fine-grained detector (FGD) system. The flux normalization is measured by the 1KT to estimate the expected number of events at SK. Since the 1KT has the same detector technology as SK, most of systematic uncertainties on the measurement are canceled. The energy spectrum is measured by analyzing the muon momentum and angular distributions in both detector systems. The 1KT has a high efficiency for reconstructing the momentum of muons below $1 \text{ GeV}/c$, and full 4π coverage in solid angle. However, the 1KT has little efficiency for reconstructing muons with momentum above $1.5 \text{ GeV}/c$ since they exit the detector. The FGD, on the other hand, has high efficiency for measuring muons above $1 \text{ GeV}/c$, and the

two complementary detectors are thus able to completely cover the relevant energy range.

In the 1KT analysis, a cylindrical fiducial volume of 25 tons oriented along the beam direction is used. Event selection criteria for the flux normalization are the same as those in reference [4]. Events which deposit more than $\sim 100 \text{ MeV}$ of energy are used for the measurement of the integrated flux. The measurement has a 5% systematic uncertainty, of which the largest contribution comes from the vertex reconstruction [4]. For the spectrum measurement, further cuts are imposed in order to select $1R\mu$ events which stop in the detector. Among the events selected for the flux normalization measurement, 53% of the events have 1 ring. The events with a muon exiting from the detector are effectively eliminated by requiring the maximum charge of any PMT to be less than 200 photo-electrons; 68% of the 1 ring events remain after this requirement. The largest systematic uncertainty for the spectrum measurement is an uncertainty on the energy scale. The energy scale is understood to within $^{+2}_{-3}\%$, which is confirmed with both cosmic-ray muons and beam-induced π^0 s.

The FGD is comprised of a scintillating fiber and water detector (SciFi) [7], a lead-glass calorimeter (LG), and a muon range detector (MRD) [8]. In the FGD analysis, events containing one or two tracks with vertex within the 5.9 ton fiducial volume of the SciFi are used. The track finding efficiency is 70% for a track passing through three layers of scintillating fiber and close to 100% for more than 5 layers [9]. Three layers is the minimum track length required in this analysis. Events which have at least one track passing into the MRD are chosen in order to select ν_μ -induced CC interactions. The momentum of the track is measured by its range through the SciFi, LG, and MRD, with accuracy of 3%.

If the proton produced in the QE interaction has a momentum greater than $600 \text{ MeV}/c$, its track may also be reconstructed. In the case where a second track is visible, the kinematic information is used to enhance the fraction of QE events in the sample. Assuming QE interaction, the direction of the proton can be predicted from the muon momentum. The QE enhanced sample is selected by requiring that the direction of the second track agrees with the prediction to within 25 degrees. Events where the direction of the second track differs from the prediction by more than 30 degrees are put into a non-QE enhanced sample. In the QE enhanced sample, 62% of the events are estimated to be QE events from the MC simulation. In the non-QE enhanced sample, 82% of events are estimated to come from interactions other than QE. The SciFi events are divided into three event categories: 1-track, 2-track QE enhanced, and 2-track non-QE enhanced samples.

The 2-dimensional distributions of the muon momentum versus angle with respect to the beam direction of four event categories (the 1KT event sample and the

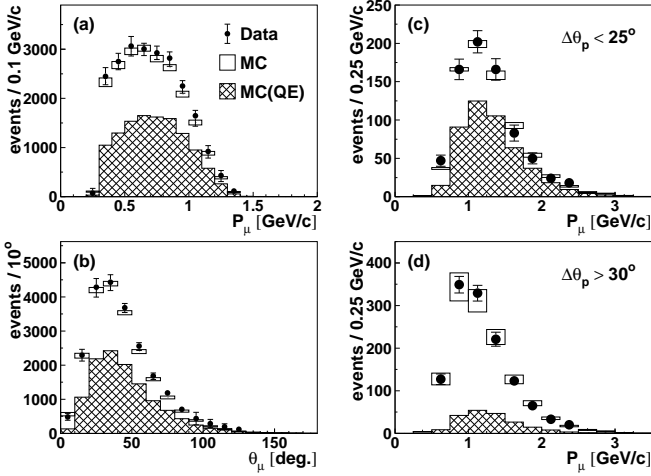


FIG. 1: (a) The muon momentum distribution of the 1KT $1R\mu$ sample, (b) the angular distribution of the 1KT $1R\mu$ sample, (c) the muon momentum distribution of the SciFi QE enhanced sample, and (d) that of the SciFi non-QE enhanced sample. The crosses are data and the boxes are MC simulation with the best fit parameters. The hatched histogram shows the QE events estimated by MC simulation.

three SciFi event samples) are used to measure the neutrino spectrum. A χ^2 -fitting method is used to compare this data against the MC expectation. The neutrino spectrum is divided into 8 energy bins as defined in Table I. During the fit, the flux in each energy bin is re-weighted relative to the values in the beam MC, and the parameter R_{nqe} is used to re-weight the ratio between the QE and non-QE cross-section relative to the MC simulation. The systematic uncertainties of the ND are incorporated into the fitting parameters. They are the energy scales, the track finding efficiencies, and the detector thresholds. In addition, the spectrum measurement by PIMON is used as a constraint on the re-weighting factors.

The value of χ^2 is 227.2/197 d.o.f. at the best fit point. All the parameters including the detector systematics are found to lie within their expected errors. The muon momentum and angular distributions of $1R\mu$ events in the 1KT, and the muon momentum distributions of the 2-track QE enhanced and non-QE enhanced events in SciFi are overlaid with the re-weighted MC in Figure 1. The fit result agrees well with the data. The errors of the measurement are provided in the form of an error matrix. Correlations between the parameters of the fit are taken into account in the oscillation analysis using this matrix. The diagonal elements in the error matrix on the determination of the spectrum at SK are shown in Table I.

The uncertainty due to neutrino interaction models is separately studied. In QE scattering, the axial vector mass in the dipole formula is set to a central value of $1.1 \text{ GeV}/c^2$ and is varied by $\pm 10\%$. The axial mass for single pion production is set to a central value of

E_ν	Φ_{ND}	F/N ratio	ϵ_{SK}
0 - 0.5	37	2.6	8.7
0.5 - 0.75	12	4.3	4.3
0.75 - 1.0	6.7	4.3	4.3
1.0 - 1.5	3.1	6.5	8.9
1.5 - 2.0	4.7	10	10
2.0 - 2.5	8.2	11	9.8
2.5 - 3.0	15	12	9.9
3.0 -	17	12	9.9

TABLE I: The percentage size of the energy dependent systematic errors on the predicted neutrino spectrum at SK. The left most column indicates the lower and the upper edges of energy bins in GeV.

$1.2 \text{ GeV}/c^2$ and is varied by $\pm 20\%$ [10]. This affects both the q^2 dependence of the cross-section and the total cross-section. For coherent pion production, two different models are compared: one is the Rein and Sehgal model [11], and the other is a model by Marteau [12]. For deep inelastic scattering, GRV94 [13] and the corrected structure function by Bodek and Yang [14] are studied. For the oscillation analysis the Marteau model and Bodek and Yang structure functions are employed. Varying the choice of models causes the fitted value of R_{nqe} ($= 0.93$) to change by $\sim 20\%$. In order to account for this, an additional systematic error of $\pm 20\%$ on R_{nqe} is added to the error matrix. The choice of models and axial mass does not affect the spectrum measurement itself beyond the size of the fitted errors.

The F/N ratio from the beam simulation is used to extrapolate the measurements at the ND to those at SK. The errors including correlations above 1 GeV, where the PIMON is sensitive, are estimated based on the PIMON measurements. The errors on the ratio for E_ν below 1 GeV are estimated based on the uncertainties in the hadron production models used in the K2K beam MC [4]. The errors on the expected neutrino spectrum at SK due to diagonal uncertainties in the error matrix for the F/N ratio are summarized in Table I.

The events in SK are selected using the timing information provided by the global positioning system. Events detected in SK must occur within an expected beam arrival time window of $1.5 \mu\text{sec}$. In addition, the detected events must have no activity in outer detector, and have an energy deposit greater than 30 MeV with a vertex reconstructed within the 22.5 kton fiducial volume [4]. This sample of events is referred to as the fully contained (FC) sample. The efficiency of this selection is 93% for CC interactions. Fifty-six events satisfy the criteria. With the timing cut, the expected number of atmospheric neutrino background is approximately 10^{-3} events.

The expected number of FC events at SK without oscillation is estimated to be $80.1^{+6.2}_{-5.4}$. The correlations between energy bins from the spectrum measurement at

the ND and the F/N ratio are taken into account in the estimation of the systematic errors. The major contributions to the errors come from the uncertainties in the F/N ratio ($^{+4.9\%}_{-5.0\%}$) and the normalization (5.0%), dominated by uncertainties of the fiducial volumes due to vertex reconstruction both at the 1KT and SK.

A two flavor neutrino oscillation analysis, with ν_μ disappearance, is performed by the maximum-likelihood method. In the analysis, both the number of FC events and the energy spectrum shape for $1R\mu$ events are used. The likelihood is defined as $\mathcal{L} = \mathcal{L}_{norm} \times \mathcal{L}_{shape}$. The normalization term $\mathcal{L}_{norm}(N_{obs}, N_{exp})$ is the Poisson probability to observe N_{obs} events when the expected number of events is $N_{exp}(\Delta m^2, \sin^2 2\theta, f)$. The symbol f represents a set of parameters constrained by the systematic errors. These parameters are described in detail later. The shape term, $\mathcal{L}_{shape} = \prod_{i=1}^{N_{1R\mu}} P(E_i; \Delta m^2, \sin^2 2\theta, f)$, is the product of the probability for each $1R\mu$ event to be observed at $E_\nu^{\text{rec}} = E_i$, where P is the normalized E_ν^{rec} distribution estimated by MC simulation and $N_{1R\mu}$ is the number of $1R\mu$ events.

In the oscillation analysis, the whole data sample is used for \mathcal{L}_{norm} , i.e. $N_{obs} = 56$. The spectrum shape in June 1999 was different from that for the rest of the running period because the target radius and horn current were different. The estimation of energy correlations in the spectrum at the ND and in the far/near ratio has not been completed for this period. Thus, data taken in June 1999 are discarded for \mathcal{L}_{shape} . The discarded data correspond to 6.5% of total POT. The number of $1R\mu$ events from the entire running period is 30, and that excluding the data of June 1999 is 29.

The parameters f consist of the re-weighted neutrino spectrum measured at the ND (Φ_{ND}), the F/N ratio, the reconstruction efficiency (ϵ_{SK}) of SK for $1R\mu$ events, the re-weighting factor for the QE/non-QE ratio R_{nqe} , the SK energy scale and the overall normalization. The errors on the first 3 items depend on the energy and have correlations between each energy bin. The diagonal parts of their error matrices are summarized in Table I. As explained earlier, the error on R_{nqe} is set to 20%. The error on the SK energy scale is 3% [15]. Two different approaches are taken for the treatment of systematic errors in the likelihood. The first is to treat the parameters f as fitting parameters with an additional constraint term in the likelihood (method 1) [1]. The other approach is to average the $\mathcal{L}(f)$ sampled over many random trials weighted according to the probability density distribution of the systematic parameters f (method 2) [16].

The likelihood is calculated at each point in the Δm^2 and $\sin^2 2\theta$ space to search for the point where the likelihood is maximized. The best fit point in the physical region of oscillation parameter space is found to be at $(\sin^2 2\theta, \Delta m^2) = (1.0, 2.8 \times 10^{-3} \text{ eV}^2)$ in method 1 and at $(1.0, 2.7 \times 10^{-3} \text{ eV}^2)$ in method 2. If the whole space including the unphysical region is consid-

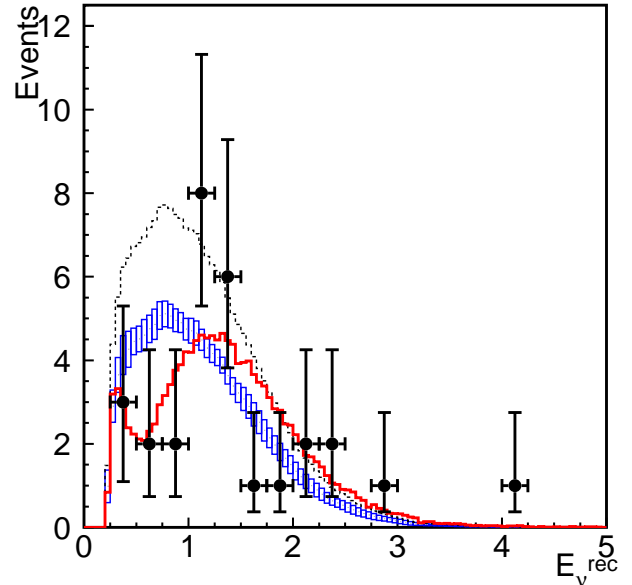


FIG. 2: The reconstructed E_ν distribution (from method 1). Points with error bars are data. Box histogram is expected spectrum without oscillations, where the height of the box is the systematic error. The solid line is the bestfit spectrum. These histograms are normalized by the number of events observed. In addition, the dashed line shows the expectation with no oscillations normalized to the expected number of events.

ered the values are $(1.03, 2.8 \times 10^{-3} \text{ eV}^2)$ in method 1 and $(1.05, 2.7 \times 10^{-3} \text{ eV}^2)$ in method 2. The results from two methods are consistent with each other. At the best fit point in the physical region the total number of predicted events is 54.2, which agrees with the observation of 56 within statistical error. The observed E_ν^{rec} distribution of the $1R\mu$ sample is shown in Fig. 2 together with the expected distributions for the best fit oscillation parameters, and the expectation without oscillations. Consistency between the observed and best-fit E_ν^{rec} spectrum is checked by using Kolmogorov-Smirnov(KS) test. A KS probability of 79% is obtained. The best fit spectrum shape agrees with the observations.

The probability that the observations are due to a statistical fluctuation instead of neutrino oscillation is estimated by computing the likelihood ratio of the no-oscillation case to the best fit point. The no-oscillation probabilities are calculated to be 0.7% and 0.4% for method 1 and 2 respectively. When only normalization (shape) information is used, the probabilities are 1.3% (16%) and 0.7% (14.3%) for the two methods. Allowed regions of oscillation parameters are evaluated by calculating the likelihood ratio of each point to the best fit point, and are drawn in Fig. 3. Both methods give essentially the same results. In order to be conservative, the result from method 1 is shown in the figure as it gives a slightly larger allowed region at the 99% C.L. The 90% C.L. contour crosses the $\sin^2 2\theta = 1$ axis at 1.5

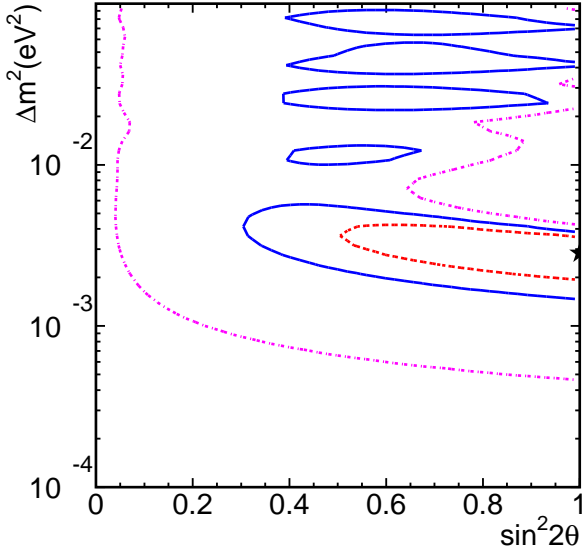


FIG. 3: Allowed regions of oscillation parameters. Dashed, solid and dot-dashed lines are 68.4%, 90% and 99% C.L. contours, respectively. The best fit point is indicated by the star.

and 3.9×10^{-3} eV 2 for Δm^2 . The oscillation parameters preferred by the total flux suppression and the energy distortions alone also agree well. Finally, the uncertainties of neutrino interactions are studied using the same procedure as the spectrum measurement at the ND. It is found that the effects of the interaction model difference on all the results are negligible due to the cancellation caused by using the same models in both the ND and SK.

In conclusion, both the number of observed neutrino events and the observed energy spectrum at SK are consistent with neutrino oscillation. The probability that the measurements at SK are explained by statistical fluctuation is less than 1%. The measured oscillation parameters are consistent with the ones suggested by atmospheric neutrinos. At the time of this letter the K2K experiment has collected approximately one-half of its planned 10^{20} protons on target.

We thank the KEK and ICRR Directorates for their strong support and encouragement. K2K is made possible by the inventiveness and the diligent efforts of the KEK-PS machine and beam channel groups. We gratefully acknowledge the cooperation of the Kamioka Mining and Smelting Company. This work has been supported by the Ministry of Education, Culture, Sports, Science and Technology, Government of Japan and its grants for Scientific Research, the Japan Society for Promotion of Science, the U.S. Department of Energy, the Korea Research Foundation, and the Korea Science and Engineering Foundation.

* For current affiliations see <http://neutino.kek.jp/present-addresses0211.ps>

- [1] Y. Fukuda et al. (Super-Kamiokande), *Phys. Rev. Lett.* **81**, 1562 (1998), hep-ex/9807003.
- [2] S. Fukuda et al. (Super-Kamiokande), *Phys. Lett.* **B539**, 179 (2002), hep-ex/0205075.
- [3] Q. Ahmad et al. (SNO), *Phys. Rev. Lett.* **89**, 011301 (2002), hep-ex/0204008.
- [4] S. H. Ahn et al. (K2K), *Phys. Lett.* **B511**, 178 (2001), hep-ex/0103001.
- [5] M. Ieiri et al. (1997), prepared for 11th Symposium on Accelerator Technology and Science, Hyogo, Japan, 21-23 Oct 1997.
- [6] T. Maruyama, Ph.D. thesis (Tohoku University) (2000).
- [7] A. Suzuki et al. (K2K), *Nucl. Instrum. Meth.* **A453**, 165 (2000), hep-ex/0004024.
- [8] T. Ishii et al. (K2K MRD Group), *Nucl. Instrum. Meth.* **A482**, 244 (2002), hep-ex/0107041.
- [9] B. J. Kim et al. (2002), hep-ex/0206041.
- [10] V. Bernard, L. Elouadrhiri, and U. G. Meissner, *J. Phys. G* **28**, R1 (2002), hep-ph/0107088.
- [11] D. Rein and L. M. Sehgal, *Nucl. Phys.* **B223**, 29 (1983).
- [12] J. Marteau et al., *Nucl. Instrum. Meth.* **A451**, 76 (2000).
- [13] M. Gluck, E. Reya, and A. Vogt, *Z. Phys.* **C67**, 433 (1995).
- [14] A. Bodek and U.-K. Yang, submitted to *Nucl. Phys. Proc. Suppl.* (2002), hep-ex/0203009.
- [15] Y. Fukuda et al. (Super-Kamiokande), *Phys. Lett.* **B433**, 9 (1998), hep-ex/9803006.
- [16] J. Swain and L. Taylor, *Nucl. Instrum. Meth.* **A411**, 153 (1998), hep-ex/9712015.